Electron Transfer Behavior and Solid State Structures of the Helical Cobalt Complexes of the Open-Chain Tetrapyrrole Ligand, Octaethylbilindione

Saeed Attar, Alan L. Balch,* Pamela M. Van Calcar, and Krzysztof Winkler†

Contribution from the Department of Chemistry, University of California, Davis, California 95616

Received August 15, 1996[⊗]

Abstract: A study of the redox behavior of the cobalt complex of octaethylbilindione (H_3OEB), a biliverdin analog, reveals that coordination of the ligand allows its complexes to undergo reversible, one-electron transfer processes, whereas the free ligand itself undergoes an irreversible two-electron oxidation. Thus, the four-membered electron transfer series involving $[Co(OEB)]^n$ with $n = +1, 0, -1, -2$ has been observed electrochemically. The most highly oxidized member of this series has been isolated in the form of its triiodide salt, $[Co^{II}(OEBOx)]I_3 \cdot 0.5CH_2Cl_2$, and characterized by X-ray diffraction. The structure involves helical coordination of the linear tetrapyrrole ligand about the cobalt with all four nitrogen atoms coordinated with Co−N distances falling in the narrow range, 1.898(7)−1.926(7) Å. The triiodide ion, which is disordered over three orientations, is ion paired to the complex. The Co···I distance (2.818 Å in the predominant orientation) is much longer than expected for a Co−I covalent bond. In the solid state, pairs of $[Co^{II}(OEBOx)]I_3$ crystallize about a center of symmetry so that two identical tab/slot arrangements, which involve CH···O hydrogen bonds, occur. These supramolecular arrangements involve hydrogen bonding between the lactam oxygen of one complex and methine and two methylene protons of an adjacent complex. Similar hydrogen bonded motifs are found in other complexes derived from octaethylbilindione and may occur for biliverdin IX derivatives as well.

Introduction

Biliverdin IXα (**1a**), which is formed by heme oxygenase through oxidative attack upon the α-methine position of heme,[1] has been suggested to have both anti-oxidant activity[2] and anti-HIV activity.[3,4] Thus, studying the chemical behavior of biliverdin and its synthetic analogs, especially in redox reactions, may lead to a better understanding of these potentially significant physiological roles. It has been previously reported that octaethylbilindione (**1b**) undergoes a facile 2-electron oxidation by diiodine to produce an oxidized tetrapyrrole cation, $[H_2OEBOx]^+$, as shown in eq 1.[5] This cation crystallizes as the salt, $[H_2OEBOx]I_3 \cdot 0.5I_2 \cdot 0.5CH_2Cl_2 \cdot 0.2C_6H_{14}$, in which two cations are paired through hydrogen bonding.

Here we are concerned with the effect that complexation of H_3OEB by metal ions will have on the redox properties of the resulting complexes. Previous work has also shown that octaethylbilindione (**1b**) is a good ligand which forms an array of complexes with manganese, iron, cobalt, nickel, and copper.[6−9] An iron complex of **1b** is a significant product in the coupled oxidation process in which an iron porphyrin is treated with dioxygen in pyridine solution in the presence of a reducing agent.[10,11] This process has been widely employed as a model for heme catabolism and the heme oxygenase reaction. Unfortunately, the iron complex of octaethylbilindione is unstable with respect to loss of iron, and this severely hampers its further study.

However, the cobalt complex, Co(OEB), **3**, is stable to both metal ion dissociation and toward dioxygen.[7] Thus, it is convenient to use **3** in further studies of the behavior of chemical and physical behavior this sort of complex. The locations of the terminal lactam oxygen atoms in this tetrapyrrole prevent the ligand from becoming planar when it coordinates to a small, first row transition metal ion. Consequently, in Co(OEB) the cobalt ion achieves nearly planar coordination, but the ligand adopts a helical geometry in which the two lactam oxygen atoms are separated by 3.116 Å. Unlike the corresponding manganese and iron complexes,[7,10] which dimerize through pairwise axial

† On leave from the Institute of Chemistry, University of Warsaw, Bialystok Branch.

⊗ Abstract published in *Advance ACS Abstracts,* March 15, 1997.

(1) **(1)** (a) O'Carra, P. In *Porphyrins and Metalloporphyrins*; Smith, K. M., Ed.; Elsevier: New York, 1975; p 123. (b) Schmid, R.; McDonagh, A. F. In *The Porphyrins*; Dolphin, D., Ed.; Academic Press: New York, 1979; Vol. 6, p 258. (c) Brown, S. B. In *Bilirubin*; Heirwegh, K. P. M., Brown, S. B., Eds.; CRC Press, Inc.: Boca Raton, FL, 1982; Vol. 2, p 1. (d) Bissell, D. M. In *Liver: Normal Function and Disease. Bile Pigments and Jaundice*; Ostrow, J. D., Ed.; Marcel Dekker, Inc.: New York, 1986; Vol. 4, p 133. (e) Maines, M. D. *Heme Oxygenase: Clinical Applications and Functions*; CRC Press: Boca Raton, FL, 1992. (f) Chang, C. K.; Avilés, G.; Bag, N. *J. Am. Chem. Soc.* **1994**, *116*, 12127.

(2) Stocker, R.; Yamamoto, Y.; McDonagh, A. F.; Glazer, A. N.; Ames, B. N. *Science* **1987**, *235*, 1043.

(3) Nakagami, T.; Taji, S.; Takahashi, M.; Yamanishi, K. *Microbiol. Immunol.* **1992**, *36*, 381.

(4) Mori, H.; Otake, T.; Morimoto, M.; Ueba, N.; Kunita, N.; Nakagami, T.; Yamasaki, N.; Taji, S. *Jpn. J. Cancer Res.* **1991**, *82*, 755.

(5) Balch, A. L.; Koerner, R.; Olmstead, M. M.; Mazzanti, M.; Safari, N.; St. Claire, T. *J. Chem. Soc., Chem. Commun.* **1995**, 643.

(6) Bonnett, R.; Buckley, D. G.; Hamzetash, D. *J. Chem. Soc., Perkin Trans I*, **1981**, 322.

(7) Balch, A. L.; Mazzanti, M.; Noll, B. C.; Olmstead, M. M. *J. Am. Chem. Soc.* **1994**, *116*, 9114.

(8) Balch, A. L.; Mazzanti, M.; Noll, B. C.; Olmstead, M. M. *J. Am. Chem. Soc.* **1993**, *115*, 12206.

(9) Bonfiglio, J. V.; Bonnett, R.; Buckley, D. G.; Hamzetash, D.; Hursthouse, M. B.; Abdul Malik, K. M.; McDonagh, A. F.; Trotter, J. *Tetrahedron* **1983**, *39*, 1865. No atomic positions for hydrogen were reported.

(10) Balch, A. L., Latos-Grażyński, L.; Noll, B. C.; Olmstead, M. M.; Safari, N. *J. Am. Chem. Soc.* **1993**, *115*, 9056.

(11) Balch, A. L.; Latos-Grażyński, L.; Noll, B. C.; Olmstead, M. M.; Szterenberg, L.; Safari, N. *J. Am. Chem. Soc.* **1993**, *115*, 1422.

S0002-7863(96)02871-5 CCC: $14.00

Chart 1

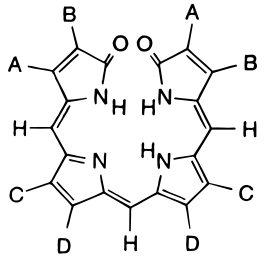

1a, A = C = Methyl
B = Vinyl
D = Propionate

1b, A = B = C = D = ethyl H_3OEB

(1)

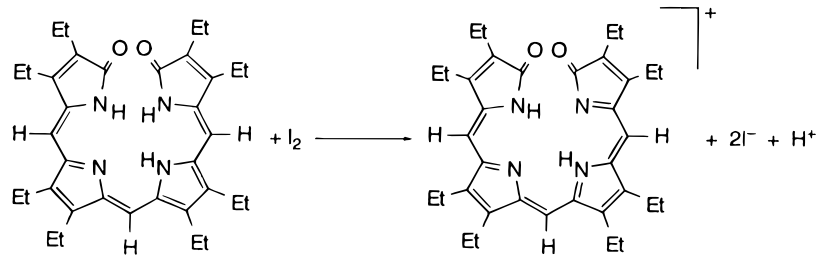

1b, H_3OEB **2**$^+$, $[H_2OEBOx]^+$

Scheme 1

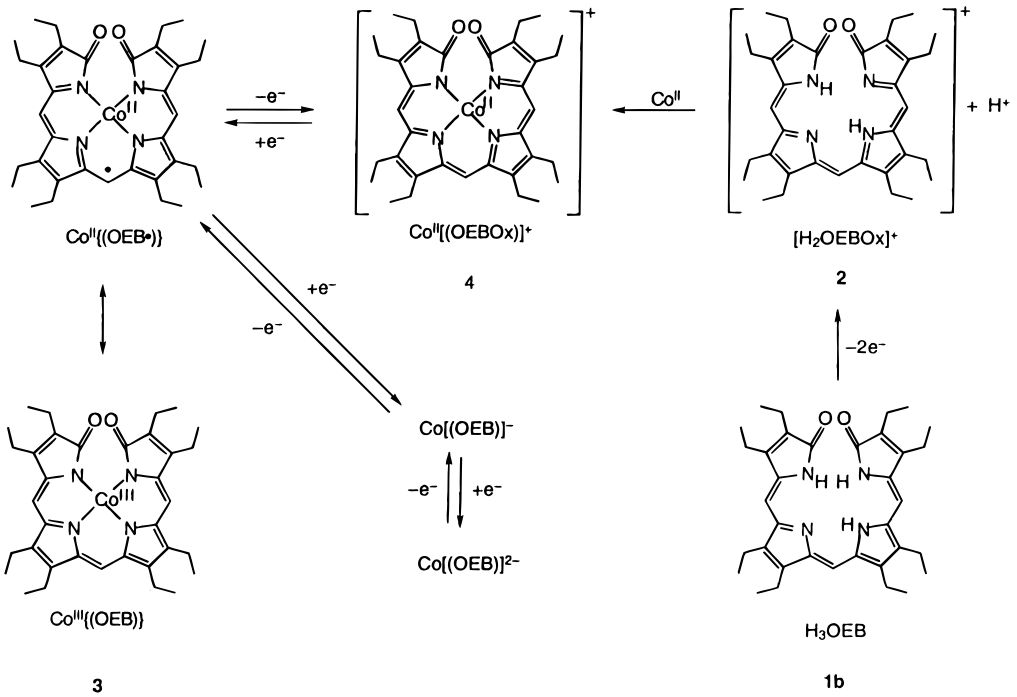

coordination of an oxygen atom from an adjacent molecule, Co(OEB) is monomeric both in solution and in the solid state.[7] The physical properties of Co(OEB), which include a remarkable ^{1}H NMR spectrum, suggest that its electronic structure is comprised of resonance components that include $Co^{III}/(OEB)^{3-}$ and $Co^{II}/(OEB^{\bullet})^{2-}$ electronic distributions (where $(OEB)^{3-}$ is the trianion obtained by deprotonation of H_3OEB and $(OEB^{\bullet})^{2-}$ is the radical dianion hypothetically obtained by one-electron oxidation of $(OEB)^{3-}$).[7]

Results and Discussion

Electrochemical and Chemical Studies. The chemical and electrochemical results described in this section are summarized in Scheme 1.

Figure 1 shows cyclic voltammetric curves and Osteryoung square-wave voltammetric data for Co(OEB) in dichloromethane solution. One reversible oxidation (at −152 mV with ΔE_p = 59(1) mV and $W_{1/2}$ = 123(2) mV) and two reversible reductions (at −784 mV with ΔE_p = 60(1) mV and $W_{1/2}$ = 122(2) mV)

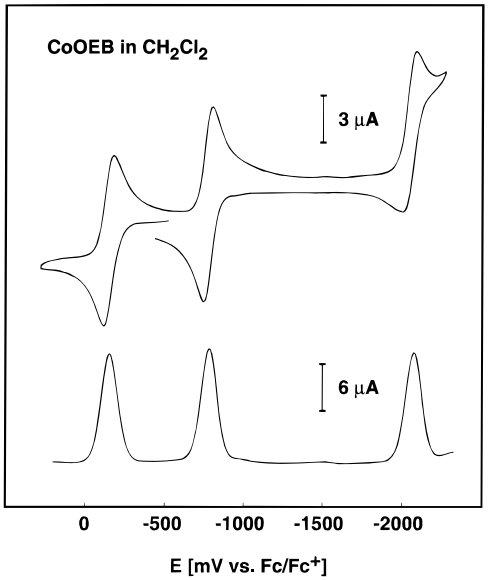

Figure 1. Cyclic voltammogram and differential pulse voltammogram of Co(OEB) (1.6 mM) in dichloromethane solution with 0.1 *M* tetra(*n*-butyl)ammonium perchlorate as supporting electrolyte.

and at −2076 mV with $\Delta E_p = 65(1)$ mV and $W_{1/2} = 126(2)$ mV) are observed. The experimental values of ΔE_p and $W_{1/2}$ are close to the theoretical values of 57 and 125 mV that are expected for reversible, one-electron processes.[12] The clean, reversible nature of the redox processes indicate that major changes in the coordination environment do not occur during the electron transfer processes. In contrast to the data shown in Figure 1, comparable electrochemical data for the free ligand, octaethylbilindione (H_3OEB), reveal an irreversible oxidation at +200 mV and an irreversible reduction at −1700 mV. Thus Co(OEB) is more easily oxidized and more easily reduced than free octaethylbilindione. As noted above the chemical oxidation of octaethylbilindione results in a two-electron oxidation.[5]

The one-electron oxidation of Co(OEB) can be accomplished chemically by the addition of either diiodine or silver hexafluorophosphate to a solution of the complex. The results of titrating a solution of diiodine in dichloromethane-d_2 into a solution of Co(OEB) in dichloromethane-d_2 are shown in Figure 2. Trace A shows the ^{1}H NMR spectrum of Co(OEB) which has been discussed previously.[7] Addition of diiodine causes a broadening and shifting of the resonances in the spectrum as shown in trace B. Addition of further quantities of diiodine results in a gradual emergence of distinct resonances and a shift of these resonances away from the diamagnetic region. After the addition of 1.5 molar equiv of diiodine, no further changes in the spectrum are seen. The changes observed are consistent with the occurrence of the following reactions.

$$\mathrm{Co(OEB)} + {}^1/_2\mathrm{I_2} \rightarrow [\mathrm{Co^{II}(OEBOx)}]\mathrm{I} \qquad (1)$$

$$[\mathrm{Co^{II}(OEBOx)}]\mathrm{I} + \mathrm{I_2} \rightarrow [\mathrm{Co^{II}(OEBOx)}]\mathrm{I_3} \qquad (2)$$

The ^{1}H NMR spectrum of $[Co^{II}(OEBOx)]I_3$, [**4**] I_3, shown in trace D reveals the presence of eight methylene resonances. Four methyl resonances occur at 5.55, 3.73, 0.49, and 0.20 ppm, with the two upfield resonances partially obscured by solvent impurities in trace D. One meso resonance is clearly present at −20 ppm. The other meso resonance coincides with the methylene resonance at 12.62 ppm. That meso resonance is more readily observed in trace C where it is found at higher field.

(12) Galus, Z. *Fundimentals of Electrochemical Analysis*, 2nd ed.; Ellis Horwood: New York, 1994; p 292.

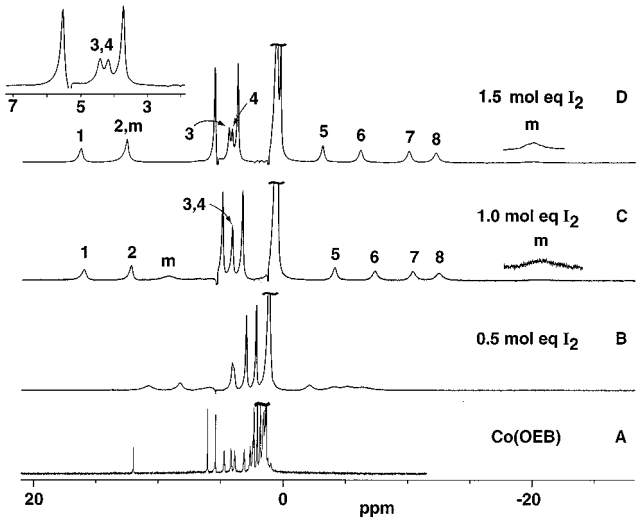

Figure 2. 300 MHz ^{1}H NMR spectra of a solution of Co(OEB) in dichloromethane-d_2 with incremental addition of diiodine. In traces C and D the eight methylene resonances are identified by the numerals, 1−8, and two meso resonances are denoted by m, respectively. The inset in trace D shows an expansion of the 7−3 ppm region where methylene resonances 3 and 4 occur. The spectra in traces B, C, and D were taken under inversion recovery conditions with a τ value of 20 ms.

The observation of only eight methylene resonances, four methyl resonances, and two meso resonances indicates that the presence of the triiodide ion makes a minor perturbation to the core of the cobalt complex. If the complex were truly five-coordinate with an anionic ligand firmly bonded to cobalt, then 16 methylene resonances, 8 methyl resonances and 3 meso resonances would be expected to appear in the ^{1}H NMR spectrum. The observations suggest that the oxidized product exists as a loose ion pair and that the triiodide ion is not coordinated to cobalt in solution.

Treatment of Co(OEB) with silver hexafluorophosphate in dichloromethane-d_2 produces changes in the ^{1}H NMR spectrum that are similar to those seen in Figure 2. The similarity in these spectra, in which either hexafluorophosphate or triiodide is the counter ion, provides further evidence that the anion is not coordinated in solution.

The oxidized complex has been isolated from diiodine treated solutions of Co(OEB). Purple crystals of $[Co^{II}(OEBOx)]I_3 \cdot 0.5CH_2Cl_2$ can be obtained by addition of pentane to a dichloromethane solution of the complex. Additionally, treatment of $[H_2OEBOx]I_3$ with cobalt(II) acetate produces a dark green solution from which $[Co^{II}(OEBOx)]I_3 \cdot 0.5CH_2Cl_2$ can be obtained.

The magnetic moment of $[Co^{II}(OEBOx)]I_3$ as determined by the Evans' method[13] in dichloromethane solution is 1.8 (2) μ_β.

The EPR spectrum of a dichloromethane solution of $[Co^{II}(OEBOx)]I_3 \cdot 0.5CH_2Cl_2$ at room temperature shows a broad (580 Gauss peak-to-peak) resonance at $g = 2.28$. Figure 3 shows the spectrum of a sample of solid $[Co^{II}(OEBOx)]I_3 \cdot 0.5CH_2Cl_2$ at 77 K. The experimental spectrum (trace A) shows a rhombic pattern that can be fit with $g_1 = 2.42$, $g_2 = 2.23$, and $g_3 = 2.01$. The computed spectrum is shown in trace B. Hyperfine coupling from cobalt is not resolved in spectra obtained in dichloromethane or from the solid. Nevertheless, the g values and line widths are consistent with previous work on the EPR spectra of low-spin Co^{II} complexes.[14−16] Thus, they are indicative of the presence of Co^{II} in the complex.

(13) Evans, D. F. *J. Chem. Soc.* **1959**, 2003.
(14) Walker, F. A. *J. Am. Chem. Soc.* **1970**, *92*, 4235.
(15) Walker, F. A. *J. Magn. Reson.* **1974**, *15*, 201.

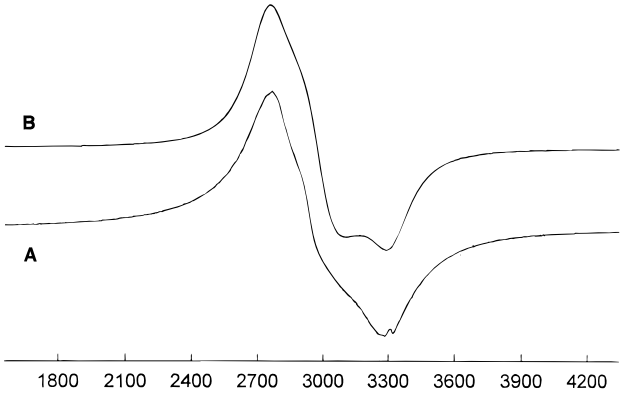

Figure 3. Trace A, experimental EPR spectrum of solid $[Co^{II}(OEBOx)]I_3 \cdot 0.5CH_2Cl_2$ at 77 K. Trace B, computed EPR spectrum with $g_1 = 2.23$, $g_2 = 2.42$, and $g_3 = 2.01$.

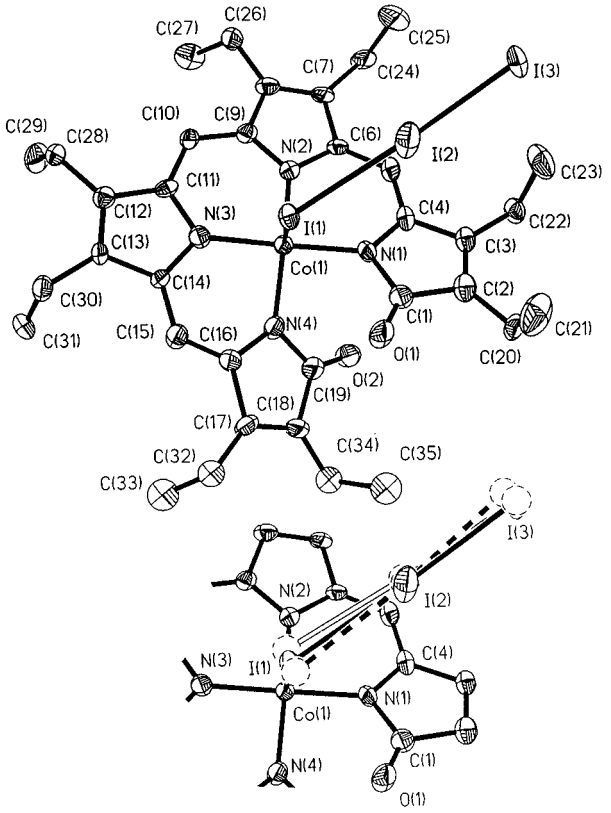

Figure 4. A perspective view of $[Co^{II}(OEBOx)]I_3 \cdot 0.5CH_2Cl_2$ with 50% thermal contours. Only the major positions of the triiodide ligand and the two disordered ethyl group (those involving C(32), C(33) and C(34), C(35)) are shown. The lower inset shows the alternate orientations of the disordered triiodide.

The Molecular Structure of $[Co^{II}(OEBOx)]I_3 \cdot 0.5CH_2Cl_2$. The structure of this oxidized complex has been determined by X-ray crystallography. A perspective view of the complex molecule is shown in Figure 4. Selected interatomic distances and angles are given in Table 1.

The molecule lacks any crystallographically imposed symmetry. There is disorder in the positions of two ethyl groups. Only the major sites for C(32) and C(33) with 0.65 occupancy and C(34) and C(35) with 0.55 occupancy are shown. There is also disorder in the location of the triiodide group. Three sites were identified: I(1), I(2), I(3) with 0.50 occupancy; I(1′), I(2′), I(3′) with 0.25 occupancy; and I(1*), I(2*), I(3*) with 0.25 occupancy. The major orientation is shown in the full molecular drawing in Figure 4, while the inset shows the relative locations of all three sites for the triiodide ion.

(16) McGarvey, B. R. *Can. J. Chem.*. **1975**, *53*, 2498.

Table 1. Selected Bond Lengths [Å] and Angles [deg] for $[Co^{II}(OEBOx)]I_3 \cdot 0.5CH_2Cl_2$

Bond Lengths [Å]			
Co(1)−N(1)	1.916(7)	Co(1)−N(2)	1.910(7)
Co(1)−N(3)	1.926(7)	Co(1)−N(4)	1.898(7)
Co(1)−I(1)	2.818(4)	Co(1)−I(1′)	2.875(10)
Co(1)−I(1*)	2.798(14)	I(1)−I(2)	2.996(8)
I(2)−I(3)	2.812(7)	I(1′)−I(2′)	2.90(2)
I(2′)−I(3′)	2.955(14)	I(1*)−I(2*)	3.00(2)
I(2*)−I(3*)	2.820(11)	O(1)−C(1)	1.196(10)
O(2)−C(19)	1.215(10)	N(1)−C(4)	1.326(10)
N(1)−C(1)	1.462(11)	N(2)−C(9)	1.358(10)
N(2)−C(6)	1.395(10)	N(3)−C(11)	1.366(10)
N(3)−C(14)	1.391(10)	N(4)−C(16)	1.360(10)
N(4)−C(19)	1.428(11)	C(1)−C(2)	1.512(12)
C(2)−C(3)	1.342(12)	C(2)−C(20)	1.480(12)
C(3)−C(4)	1.488(11)	C(4)−C(5)	1.402(12)
C(5)−C(6)	1.368(11)	C(6)−C(7)	1.461(11)
C(7)−(8)	1.352(12)	C(8)−C(9)	1.462(11)
C(9)−C(10)	1.390(11)	C(10)−C(11)	1.380(11)
C(11)−C(12)	1.456(11)	C(12)−C(13)	1.350(11)
C(13)−C(14)	1.452(10)	C(14)−C(15)	1.379(11)
C(15)−C(16)	1.362(12)	C(16)−C(17)	1.498(12)
C(17)−C(18)	1.318(13)		
Bond Angles [deg]			
N(4)−Co(1)−N(2)	158.6(3)	N(4)−Co(1)−N(1)	92.0(3)
N(2)−Co(1)−N(1)	90.3(3)	N(4)−Co(1)−N(3)	89.0(3)
N(2)−Co(1)−N(3)	91.1(3)	N(1)−Co(1)−N(3)	173.4(3)
N(4)−Co(1)−I(1*)	97.3(4)	N(2)−Co(1)−I(1*)	104.1(4)
N(1)−Co(1)−I(1*)	84.8(4)	N(3)−Co(1)−I(1*)	88.6(4)
N(4)−Co(1)−I(1)	100.7(3)	N(2)−Co(1)−I(1)	100.6(3)
N(1)−Co(1)−I(1)	87.6(2)	N(3)−Co(1)−I(1)	85.8(2)
N(4)−Co(1)−I(1′)	106.4(3)	N(2)−Co(1)−I(1′)	94.9(3)
N(1)−Co(1)−I(1′)	89.3(3)	N(3)−Co(1)−I(1′)	84.2(3)
Co(1)−I(1)−I(2)	105.9(2)	I(3)−I(2)−I(1)	176.2(3)
Co(1)−I(1′)−I(2′)	104.2(4)	I(1′)−I(2′)−I(3′)	162.4(5)
Co(1)−I(1*)−I(2*)	104.6(5)	I(3*)−I(2*)−I(1*)	176.6(5)
C(4)−N(1)−C(1)	105.9(7)	C(4)−N(1)−Co(1)	130.2(6)
C(1)−N(1)−Co(1)	123.9(5)	C(9)−N(2)−C(6)	105.9(7)
C(9)−N(2)−Co(1)	127.2(6)	C(6)−N(2)−Co(1)	126.8(5)
C(11)−N(3)−C(14)	105.4(7)	C(11)−N(3)−Co(1)	128.5(6)
C(14)−N(3)−Co(1)	125.2(5)	C(16)−N(4)−C(19)	105.5(7)
C(16)−N(4)−Co(1)	127.7(6)	C(19)−N(4)−Co(1)	126.7(6)
O(1)−C(1)−N(1)	125.8(8)	O(1)−C(1)−C(2)	126.6(8)
N(1)−C(1)−C(2)	107.5(7)	C(3)−C(2)−C(20)	131.6(8)
C(3)−C(2)−C(1)	106.5(8)	C(20)−C(2)−C(1)	121.7(8)
C(2)−C(3)−C(4)	107.8(7)	N(1)−C(4)−C(5)	122.9(7)
N(1)−C(4)−C(3)	112.1(7)	C(5)−C(4)−C(3)	124.9(7)
C(6)−C(5)−C(4)	123.8(7)	C(5)−C(6)−N(2)	124.3(7)
C(5)−C(6)−C(7)	126.0(7)	N(2)−C(6)−C(7)	109.7(7)
C(8)−C(7)−C(6)	106.8(7)	C(8)−C(7)−C(24)	129.3(8)
C(7)−C(8)−C(9)	106.8(7)	N(2)−C(9)−C(10)	125.4(7)
N(2)−C(9)−C(8)	110.8(7)	C(10)−C(9)−C(8)	123.8(7)
C(11)−C(10)−C(9)	123.5(8)	N(3)−C(11)−C(10)	123.2(8)
N(3)−C(11)−C(12)	111.0(7)	C(10)−C(11)−C(12)	125.8(7)
C(13)−C(12)−C(11)	106.4(7)	C(12)−C(13)−C(14)	107.3(7)
C(15)−C(14)−N(3)	123.6(7)	C(15)−C(14)−C(13)	126.5(7)
N(3)−C(14)−C(13)	109.8(7)	C(16)−C(15)−C(14)	123.5(8)
N(4)−C(16)−C(15)	122.9(8)	N(4)−C(16)−C(17)	110.3(8)
C(15)−C(16)−C(17)	126.8(8)	C(18)−C(17)−C(16)	107.1(8)
C(17)−C(18)−C(19)	108.0(8)	O(2)−C(19)−N(4)	124.6(8)
O(2)−C(19)−C(18)	127.6(9)	N(4)−C(19)−C(18)	107.8(8)

The cobalt atom is bonded to the four nitrogen atoms of the tetrapyrrole ligand. A triiodide ion also lies in close proximity to the cobalt atom. The four Co−N distances (1.898(7), 1.910(7), 1.916(7), 1.926(7) Å) span a narrow range which is similar to that found for the Co−N distances (1.873(3), 1.909(3) Å) in Co(OEB). The predominant Co−I(1) distance is 2.818(4) Å, while the other two less populated sites have lengths of 2.875(10) for Co−I(1′) and 2.798(14) for Co−I(1*). These distances are all considerably longer than the Co−I distances observed in cobalt compounds with simple iodide (rather than triiodide) coordination. The average Co−I distance found for 18 com-

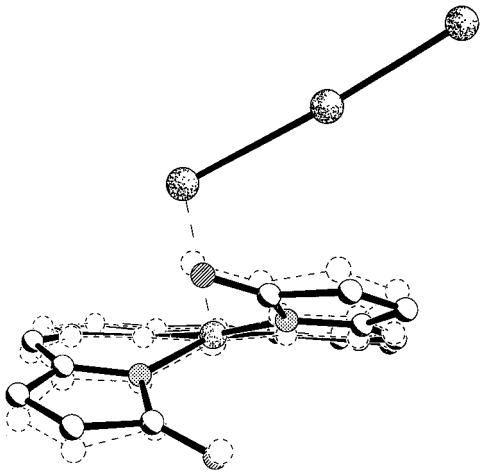

Figure 5. A superposition of the core structure of Co(OEB), shown as dashed lines, on the corresponding portion of $[Co^{II}(OEBOx)]I_3$.

pounds in the Cambridge Structural Database (CSD)[17] with a CoN_4I core is 2.589 Å. The Co−I bond lengths in $[Co^{II}(OEBOx)]I_3$ also exceed the range of Co−I distances (2.523−2.697 Å) found in those 18 compounds. Thus the lengths of the Co−I distances in $[Co^{II}(OEBOx)]I_3$ and the disorder in the location of the triiodide suggest that in the solid state this anion is weakly coordinated at best.

Within the triiodide ligand, the I−I distances, which range from 2.812(7) to 3.00(2) Å, are normal and cluster about the average I−I distance of 2.937 found in the CSD for 365 I−I distances in I_x chains where $x \geq 3$.

The helical tetrapyrrole ligands in $[Co^{II}(OEBOx)]I_3$ and Co(OEB) are compared in Figure 5. The core of $[Co^{II}(OEBOx)]I_3$ is shown with solid lines, while that of Co(OEB) is indicated by dashed contours. In both molecules, the tetrapyrrole ligands possess closely related, helical structures. For $[Co^{II}(OEBOx)]I_3$, oxidation and the approach of the triiodide ion have brought about a slight compression of the helical twist of the molecule. However, it is notable that the approach of the triiodide has introduced relatively little asymmetry to the two faces of the tetrapyrrole. What asymmetry is present is most notably observed in the trans−N−Co−N angle. In Co(OEB) these are equal (162.0(2)°), but in $[Co^{II}(OEBOx)]I_3$ the N(1)−Co−N(3) angle is widened to 173.4(3)°, while the N(4)−Co(1)−N(2) angle is somewhat compressed to 158.6(3)°.

Intermolecular Packing of $[Co^{II}(OEBOx)]I_3$ and Related Molecules in the Solid State. A common structural element comprised of C−H···O hydrogen bonds is found in the solid state structures of $[Co^{II}(OEBOx)]I_3$, M(OEB), (M = Co, Ni, Cu), and $(py)Mn^{III}(OEB)$. That structural unit, which involves a tab/slot interaction between the lactam oxygen of one molecule with a pocket of three C−H hydrogen bond donors of another molecule, is shown in Figure 6. The three donors are a meso−methine proton and protons from the two immediately adjacent methylene groups. Table 2 presents distances and angles for these tab/slot arrangements in $[Co^{II}(OEBOx)]I_3$ and other, related complexes.

In the solid state, pairs of $[Co^{II}(OEBOx)]I_3$ crystallize about a center of symmetry as shown in Figure 7. In this supramolecular arrangement, two of the motifs shown in Figure 6 occur. Only one of the lactam oxygen atoms in each tetrapyrrole ligand participates in this hydrogen bonding arrangement, since the proximity of the triiodide ion to the other lactam oxygen blocks access to that oxygen atom.

(17) Allen, F. H.; Kennard, O. *Chemical Design Automation News* **1993**, *8*, 1.

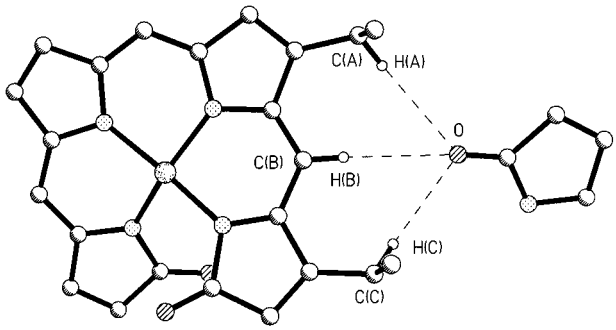

Figure 6. An idealized drawing which shows the intermolecular hydrogen bonding motif that involves the amide oxygen of one molecule and the meso C−H group and the two flanking methylene hydrogen atoms of a second molecule.

The multipoint recognition that is present in the supramolecular unit shown in Figure 6 enhances its stability and makes it a common structural element that recurs in the crystal structures of several complexes that are derived from octaethylbilindione. The centrosymmetric pair of $(py)Mn^{III}(OEB)$ molecules shown in Figure 8 is similar in supramolecular architecture to that of pairs of $[Co^{II}(OEBOx)]I_3$, which are shown in Figure 7. The absence of additional ligation or ion pairing in the four-coordinate Co(OEB) and in the isomorphic Cu(OEB) and Ni(OEB) facilitates hydrogen bonding by both lactam oxygen atoms in each tetrapyrrole ligand. In these molecular solids, linear hydrogen-bonded chains, rather than simple pairs of complexes, form. Figure 9 shows a view of the linear chain found for Co(OEB). Here the hydrogen bonding arrangement shown in Figure 6 is repeated at both ends of the helical tetrapyrrole ligand.

Examination of the hydrogen bonding parameters presented in Table 2 shows that, for each example, all of the C···O distances involved in these arrangements are <3.6 Å and many are less than 3.5 Å. Thus the C···O distances are consistent with previously determined cases of C−H···O hydrogen bonds.[18−21]

Discussion

This work shows that metal complexes of the linear tetrapyrrole, H_3OEB, like those of porphyrins, can undergo facile one-electron transfer reactions. For the cobalt complexes obtained from octaethylbilindione, a four-membered electron transfer series that involves $[Co^{II}(OEBOx)]^+$, Co(OEB), $[Co(OEB)]^-$, and $[Co(OEB)]^{2-}$ has been observed. The two most highly oxidized members, $[Co^{II}(OEBOx)]^+$ and Co(OEB), have been isolated and characterized by single crystal X-ray diffraction. Electron transfer between these two complexes is rapid on the NMR time scale. During the redox titration shown in Figure 2 only a single set of averaged resonances for the two species is observed. This observation and the reversible electrochemical behavior are consistent with the structural work which reveals only a modest differences in the geometry of the helical cores of $[Co^{II}(OEBOx)]^+$ and Co(OEB). If electron transfer between the oxidized and reduced forms of the complex were slow (as might be the case if an axial ligand were strongly bound in one form and not the other), then separate ^1H NMR resonances for the two forms would be observed. In contrast to these reversible redox processes, the free ligand undergoes irreversible oxidation and reduction at potentials that make both oxidation and reduction of H_3OEB more difficult than those of

(18) Taylor, R.; Kennard, O. *J. Am. Chem. Soc.* **1982**, *104*, 5063.
(19) Sarma, J. A. R. P.; Desiraju, G. R. *Acc. Chem. Res.* **1986**, *19*, 222.
(20) Desiraju, G. R. *Acc. Chem. Res.* **1991**, *24*, 290.
(21) Desiraju, G. R. *Acc. Chem. Res.* **1996**, *29*, 441.

Table 2. Hydrogen Bonding Parameters in Solid State Aggregation of Octaethylbilindione Derived Complexes

distance[a]	[Co(OEBOx)]I_3	pyMn(OEB)	Co(OEB)	Cu(OEB)	Ni(OEB)
O−Ha	2.70 Å	2.40 Å	2.73 Å	2.58 Å	
O−Hb	2.65 Å	2.40 Å	2.44 Å	2.45 Å	
O−Hc	2.55 Å	2.65 Å	2.50 Å	2.55 Å	
O−Ca	3.574 Å	3.251 Å	3.576 Å	3.434 Å	3.578 Å
O−Cb	3.576 Å	3.344 Å	3.399 Å	3.401 Å	3.454 Å
O−Cc	3.414 Å	3.579 Å	3.318 Å	3.341 Å	3.361 Å
O−Ha−Oa	150°	147°	148°	147°	
O−Hb−Ob	172°	168°	173°	176°	
O−Hc−Cc	149°	163°	143°	141°	
ref	this work	7	7	8	6

[a] As defined in Figure 5.

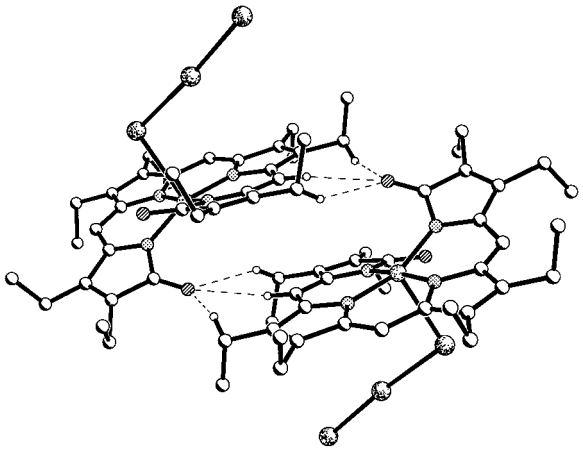

Figure 7. View of a centrosymmetric dimer formed by intermolecular contacts through hydrogen bonds (dashed lines) in [Co^{II}(OEBOx)]I_3·0.5CH_2Cl_2.

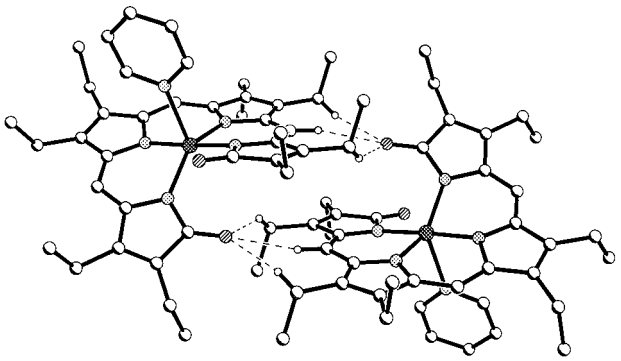

Figure 8. View of a centrosymmetric dimer formed by intermolecular contacts through hydrogen bonds (dashed lines) in (py)Mn^{III}(OEB).

Co(OEB). Thus coordination brings about a significant change in the redox behavior of this biliverdin analog. Although biliverdin has been observed in coordinated form in nature, *i.e.*, the zinc biliverdin complex found in bird's eggs,[22] it remains to be seen how metalation of biliverdin IXα affects its biochemical behavior.

The structural and spectroscopic data presented here, especially the EPR spectra and the nearly planar, four-coordinate geometry, are consistent with the formulation of the most highly oxidized member of this electron transfer series as a complex of Co^{II}, *i.e.*, $[Co^{II}(OEBOx)]^+$. The electronic structure of Co(OEB) has been discussed previously in terms of contributions from the resonance structures shown in Scheme 1. Further work is necessary to ascertain information on the electronic distribution in the reduced forms, $[Co(OEB)]^-$, and $[Co(OEB)]^{2-}$.

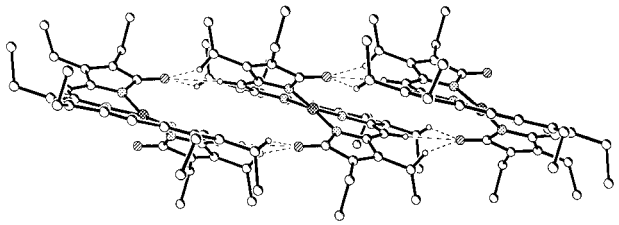

Figure 9. View of a linear chain of Co(OEB) molecules that associate by means of intermolecular contacts through hydrogen bonds (dashed lines). Similar chains are found in crystals of Ni(OEB) and Cu(OEB).

However, it appears likely that $[Co(OEB)]^-$ will contain Co^{II} and $(OEB)^{3-}$.

In the solid state, complexes derived from H_3OEB or $[H_2OEBOx]^+$ form supramolecular arrays in a common fashion that involves association through the tab/slot scheme shown in Figure 6. This packing arrangement can result in the formation of discrete pair of molecules or ions that form about a center of symmetry with only one lactam oxygen of each ligand participating in hydrogen bonding. Alternatively, a linear chain of complexes can form in which both lactam oxygen atoms function as hydrogen bond acceptors. Since centrosymmetric arrangements are involved in both cases; the pairs of complexes or linear chains contain equal numbers of helical complexes with opposite senses chirality. Thus, crystallization produces a racemic mixture within each solid. The tab/slot motif seen in Figure 6 may also be important in the supramolecular structural organization of biliverdin IX derivatives; since the meso groups in biliverdin IX have similar environments that can participate in the tab/slot interaction shown in Figure 6.

Experimental Section

Preparation of Compounds: H_3OEB (1b). The compound was prepared via the coupled oxidation of Co(OEP), as previously reported, in 50% yield.[23]

[H_2OEBOx]I_3 (2). This was prepared according to the previously reported[5] method in 72% yield.

[Co^{II}(OEBOx)]I_3, [4]I_3. Method 1, Insertion of Co^{II} into [H_2OEBOx]I_3. $[H_2OEBOx]^+I_3^-$ (70.3 mg, 0.0752 mmol) was dissolved in 20 mL of a 1:1 mixture of chloroform/ethanol to give a dark green solution. $Co(OAc)_2$·4H_2O (150 mg, 0.602 mmol) was partially dissolved in 10 mL of ethanol and added to the above green solution. The mixture was warmed in a 60 °C water-bath for 5 min and then stirred at room temperature for 20 min. Removal of solvents gave a dark green paste, which was redissolved in chloroform. A red precipitate (possibly cobalt(II) iodide) was formed and removed by gravity-filtration. The filtrate was washed with water, dried over anhydrous sodium sulfate, and gravity-filtered to remove the solid. Removal of chloroform gave a dark green paste, which was purified by crystallization from benzene/*n*-pentane: yield; 38.5 mg, 51.6%. Purple prisms of [Co^{II}(OEBOx)]I_3·0.5CH_2Cl_2, suitable for X-ray

(22) Fox, H. M.; Vevers, G. *The Nature of Animal Colors*; MacMillan Co.: New York, 1960; p 102.

(23) Balch, A. L. Mazzanti, M. St. Claire, T. M.; Olmstead, M. M. *Inorg. Chem.* **1995**, *34*, 2194.

crystallography, were obtained by diffusion of a layer of *n*-pentane into a dichloromethane solution of the complex. UV/vis data from dichloromethane solution: λ_{max}, nm, (ϵ, mol^{-1} cm^{-1}); 294 (51 900), 360 (34 500), 610 (9600).

Method 2, Addition of I_2 to Co(OEB). Co(OEB) was prepared according to the previously reposted method in 37% yield.[18] A deep purple solution of diiodine (25.4 mg, 0.10 mmol) in 10 mL of dichloromethane was added to a dark green solution of Co(OEB) (30.5 mg, 0.050 mmol) in 10 mL of dichloromethane. The mixture was stirred for 15 min, and then the volume of the solution was reduced to 4 mL. *n*-Pentane was then carefully layered over the solution. On standing overnight, purple-green crystals of the product formed. These were collected by filtration, washed with pentane, and vacuum dried: yield; 42.0 mg, 84.6%. The spectroscopic properties of the compound obtained by either method were identical.

Instrumentation. ^{1}H NMR spectra were recorded on a General Electric QE-300 FT spectrometer operating in the quadrature mode (^{1}H frequency is 300 MHz). The spectra were collected over a 20-kHz bandwidth with 8K complex data points and a 6-μs 90° pulse. For a typical spectrum, between 200 and 500 transients were accumulated with a 100-ms delay time. The signal-to-noise ratio was improved by apodization of the free induction decay. The resonance of the residual protons in dichloromethane-d_2 at 5.32 ppm was used as a secondary reference. To observe the methyl resonances that were obscured by signals in the 0.5−1.0 ppm region an inversion recovery sequence (Super-WEFT) was used with τ values varying between 1 and 200 ms.[24] Magnetic moments from solutions were obtained by the Evans' method.[12] Electronic spectra were obtained using a Hewlett-Packard diode array spectrometer. EPR spectra were obtained through the use of a Brucker ECS 106 electron spin resonance spectrometer which operated at X-band. The simulation of the EPR spectrum was carried out with the use of second-order perturbation calculations that were developed earlier[25] and modified to be consistent with $I = 7/2$. Nuclear quadrupole structure was not considered.

Cyclic Voltammetry. DC-cyclic and Osteryoung square-wave voltammetry were performed using the BAS CV-50W potentiostat in a three-electrode cell. The working electrode was a gold wire (Bioanalytical system) with a diameter of 1.5 mm. Before each experiment the electrode was polished with fine carborundum paper and 0.5 μm alumina slurry in sequence. The electrode was then sonicated in order to remove the traces of alumina from the surface, washed with water, and dried. A silver wire immersed in 0.01 M $AgClO_4$ and 0.09 M tetra(*n*-butyl)ammonium perchlorate (TBAP) in acetonitrile and separated from the working solution by a ceramic tip (Bioanalytical system) served as the reference electrode. Potentials are expressed by reference to the ferrocene/ferrocenium redox system. The counter electrode was a platinum tab with an area of ~0.5 cm^2. Tetra(*n*-butyl)ammonium perchlorate (0.1 M) served as the supporting electrode.

X-ray Data Collection. A crystal of $[Co^{II}(OEBOx)]I_3 \cdot 0.5CH_2Cl_2$ was coated with paraffin oil and mounted on a glass fiber in a 130(2) K dinitrogen stream of a Siemens R3m/v diffractometer that was equipped with a locally modified Enraf Nonius low temperature apparatus. Cell dimensions were determined by least square refinement of 35 reflections in the range of 30° < 2Θ < 40°. A total of 9465 scans were collected at 8°/min with a scan range of 1.0°. Lorenz and polarization corrections were applied. Crystal data are given in Table 3.

Table 3. Crystallographic Data for $[Co^{II}(OEBOx)]I_3 \cdot 0.5CH_2Cl_2$

formula	$C_{35.5}H_{44}ClCoI_3N_4O_2$
fw	1033.83
crystal system	monoclinic
space group	*C*2/*c*
a, Å	25.053(7)
b, Å	17.256(4)
c, Å	18.161(4)
β, deg	95.16(2)
V, Å^3	7819(3)
Z	8
T, K	130(2)
λ, Å	0.71073 (Mo Kα)
ρ, g/cm^3	1.756
μ, mm^{-1}	2.911
R_1 (obsd data)[a]	0.0678
wR_2 (all data, F^2 refinement)[a]	0.1827

[a] $$R_1 = \frac{\sum||F_o| - |F_c||}{\sum|F_o|}; \; wR_2 = \sqrt{\frac{\sum[w(F_o^2 - F_c^2)^2]}{\sum[w(F_o^2)^2]}}$$

Solution Structure and Refinement. The solution and refinement were done by use of the SHELXTL 5.01 family of programs. The structure was solved in the space group *C*2/*c* through direct methods. Refinement was done using full-matrix least squares based on F^2. An absorption correction was applied with the program XABS2.[26] Hydrogen atoms were refined by use of a riding model.

The triiodide ion is disordered over three sites. The site occupancies were determined from the difference map at 50% for I1, I2, and I3 and at 25% for I1′, I2′, I3′, I1*, I2*, and I3*. Two of the ethyl groups are also disordered. The site occupancies were refined to 0.35(2) for C32A and C33A, 0.65(2) for C32 and C33, 0.55(5) for C34 and C35, and 0.45(5) for C34A and C35A. The dichloromethane molecule was refined with a fixed C−Cl bond length of 1.77 Å and a Cl−Cl distance of 2.89 Å. A difference peak (2.003 eÅ^{-3}, 0.40 Å from the chlorine atom) suggests slight disorder in the position of the dichloromethane molecule, but attempts to model this were unstable. All non-hydrogen atoms were refined anisotropically except for the minor components of the triiodide disorder, the disordered ethyl groups, and the solvate molecule.

Acknowledgment. We thank the National Institutes of Health (Grant GM26226) for support and Dr. A. Ozarowski and Richard Koerner for advice and experimental assistance.

Supporting Information Available: For $[Co^{II}(OEBOx)]I_3 \cdot 0.5CH_2Cl_2$ a full listing of data collection and structure refinement details, atomic coordinates, bond distances and angles, anisotropic thermal parameters, hydrogen atom coordinates, and a view of the complex that shows the disorder in the ethyl group locations (13 pages). See any current masthead page for ordering and Internet access instructions.

JA9628718

(24) Inubushi, T.; Becker, E. D. *J. Magn. Reson.* **1983**, *51*, 128.
(25) Sakaguchi, U.; Arata, Y.; Fujiwara, S. *J. Magn. Reson*. **1973**, *9*, 118.
(26) XABS2: An empirical absorption correction program. Parkins, S.; Moezzi, B.; Hope, H. *J. Appl. Cryst.* **1995**, *28*, 53.